INTRODUCING A NEW 3 LEGGED 6-DOF UPS PARALLEL MECHANISM

G.R. VOSSOUGHI, M.H. ABEDINNASAB & O. AGHABABAI
Mechanical Engineering Dept., CEDRA[1]
Sharif University of Technology
Tehran, Iran

Abstract: - In this paper, we propose a new 6-DOF parallel mechanism. Due to the fact that degrees of freedom in this robot outnumber the number of kinematic chains, it is not a fully parallel mechanism. This results in a weight and inertia reduction and better dynamic performance, making it ideal for haptic and pole climbing applications. The fact that the mechanism is open on one side enable it to wrap around a pole from one side minimizing the center of gravity distance from the pole and the resulting gripping moments. Both inverse and forward Kinematic and dynamic analysis of the proposed mechanism is addressed. Workspace of the mechanism is compared to that of the Stewart's mechanism and the results show better performance. Jacobian matrix has also been determined and singular points have been discussed. Finally, the simulation results have also been validated using Matlab's SimMechanics™ Toolbox.

Key-Words: - parallel mechanisms, kinematics, Jacobian matrix, singularity analysis and dynamics

1 Introduction

Over the last two decades, parallel mechanisms have attracted the attention of several researchers. Parallel mechanisms are characterized by several kinematic chains connecting the base to the end effector, which allows the actuators to be located on or near the base of the mechanism, thereby increasing the load-carrying capacity and leading to very good dynamic properties, high accuracy and high stiffness [1].

However, since the kinematic and dynamic modeling of parallel mechanisms is far more complex than that of serial mechanisms, several issues remain open. For instance, the characterization of the singular configurations and the determination of the singularity loci are still current research topics [2].

Parallel mechanisms have first been introduced by Gough and Whitehall in tire-testing equipment [3]. Later, Stewart [4] proposed to use a parallel mechanism as a motion base for a flight simulator. The rationale for the use of this type of mechanism was its high stiffness and dexterity required to impart large accelerations to a heavy load-the cockpit of an aircraft-with six degrees of freedom. Parallel mechanisms have also been used in a number of other applications.

Haptic is the science of touch and haptic interfaces are robots that provide information to people by manipulating them [5]. Especially interesting is the application of parallel structures as haptic devices. Several examples, like the 3 degrees of freedom spherical mechanisms [6], cable-driven mechanisms Videt [7] or mechanisms with legs of several links have been presented during last years. All these devices try to explore the special characteristics of parallel structures, like low inertia, high rigidity, compactness, precise resolution and high load/power ratio, compared with serial mechanisms. However, some of these parallel haptic devices that have been developed so far still have disadvantages such as small workspace.

However, it is known that parallel mechanisms have many singularities that deteriorate force reflection performance in haptic applications. At singular points, haptic system can not generate reflecting force completely, and moreover, actuator saturation happens [8]. But, as it will be shown, in this regard our new mechanism, is highly suitable for haptic applications .

2 Geometric description

The proposed mechanism is actuated by the 3 rotary and 3 linear actuators. The rotary actuators are situated on the 3 corners (A_i) of a base platform and their shafts are connected to the lower part of the linear actuators through

[1] Center of Excellence in Design, Robotics and Automation

a universal joint. The upper part of the linear actuators is connected to the upper platform using spherical joints (B_i), see Fig. 1.

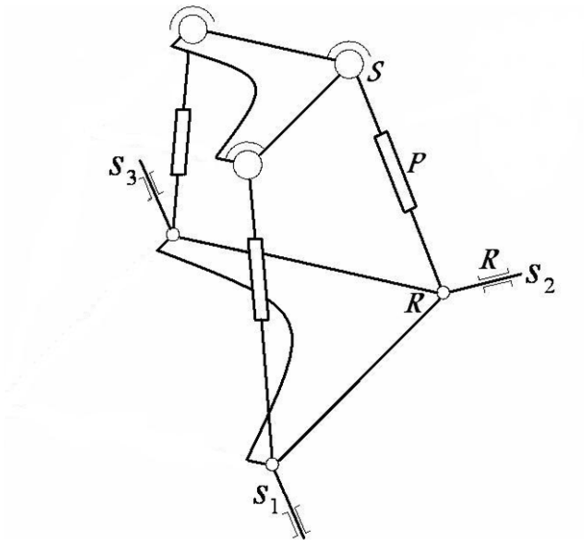

Fig. 1: Schematic of the mechanism

Cartesian coordinates $A(O,x,y,z)$ and $B(P,u,v,w)$ are connected to the base and upper platforms. Coordinates $C_i(A_i,x_i,y_i,z_i)$ have also been shown in the Fig. 2. Moreover rotary shafts are in S_i directions. $\vec{l}_i$ is the unit vector across $\overrightarrow{A_iB_i}$. Length of the lower and upper parts of the linear actuators are $2e_1$ and $2e_2$, respectively.

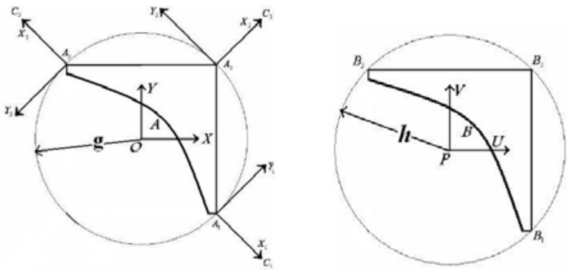

Fig. 2: Fixed and moving platforms

Assuming that each limb is connected to the fixed base by a universal joint, the orientation of limb i with respect to the fixed base can be described by two Euler angles, namely a rotation of θ_i about the rotary shaft, followed by another rotation of ψ_i about the another axis (Fig. 3).

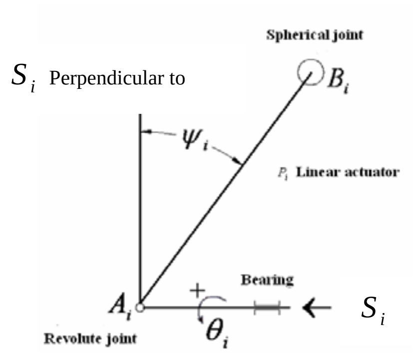

Fig. 3: Universal joint

The notations used is as follow :

${}^iJ_{1i}$, ${}^iJ_{2i}$: Link Jacobian matrix for the lower part and the upper part of the linear actuator expressed in their coordinates, respectively.

J_{S_i} : Link Jacobian matrix for the rotary actuator expressed in its coordinate.

$\vec{v}_{bi}$: The velocity of a ball point B_i.

${}^i\vec{v}_{bi}$: Transformed $\vec{v}_{bi}$ to the i th limb fame.

${}^i\vec{\omega}_i$: The angular velocity of limb i.

$\dot{\vec{v}}_{bi}$: The acceleration of the ball point B_i, expressed in the fixed frame.

${}^i\dot{\vec{v}}_{bi}$: Expresses $\dot{\vec{v}}_{bi}$ in the i th limb frame.

${}^i\dot{\vec{\omega}}_i$: The angular acceleration of limb i.

${}^i\dot{\vec{v}}_{1i}$, ${}^i\dot{\vec{v}}_{2i}$: The accelerations of the centers of mass of the i th lower and upper parts of the linear actuators, respectively.

In the 6 leg Stewart like mechanisms, the workspace is constructed by intersecting 6 spheres. But in the proposed mechanism, the workspace is constructed by intersecting of just 3 spheres. This results in a much more larger workspace for the proposed mechanism.

The placement of active joints, makes this structure unique. Placement of the 3 rotary actuators on the base platform makes this mechanism much lighter, resulting in higher achievable accelerations due to smaller inertial effects.

The proposed mechanism is ideal for haptic application and simulating high force manufacturing processes such as 3 dimensional grinding, carving and other similar processes. Also since the proposed mechanism is open on one side, it can encircle poles and it thus provides a good solution for pole climbing and manipulating robots which can travel along tubular and tree like structures with bends and branches.

3 Inverse kinematics

Perhaps the first concern in studying the kinematics of mechanisms is the number of degrees of freedom. If we use Grubler criterion, it can be seen that this is a 6-DOF mechanism. Due to the fact that degrees of freedom in this mechanism outnumber the kinematic chains, unlike Stewart platform, it is not a fully parallel mechanism. This results in a weight and inertia reduction and better dynamic performance.

There are two types of kinematic analysis problems: inverse kinematics and forward kinematics.

For the inverse kinematics, the position and orientation of the moving platform are given, and the length of the linear actuators (d_i) and the rotation of active angle (θ_i) are to be found.

$\vec{q}_i$ and $\vec{p}$ are the position of B_i and P in the reference frame A.

$$\vec{p} = \begin{bmatrix} x & y & z \end{bmatrix}^T \tag{1}$$

$$\vec{q}_i = \vec{p} + {}^A_B R \cdot \vec{b}_i \quad , \quad \vec{b}_i = \overrightarrow{OB_i} \tag{2}$$

${}^A_B R$ in equation (2) is the transformation matrix from coordinate B to A.

The length of linear actuators is then:

$$d_i^2 = (\vec{q}_i - \vec{a}_i)^T \cdot (\vec{q}_i - \vec{a}_i) \quad , \quad i = 1,2,3 \tag{3}$$

$$\vec{a}_i = \overrightarrow{OA_i} \; , \; \vec{c}_i = \frac{\vec{a}_i}{|\vec{a}_i|} \; , \; \vec{l}_i = \frac{\overrightarrow{A_i B_i}}{d_i} \tag{4}$$

R_i^t is the transformation matrix between Cartesian coordinates C_i and coordinates which their z axis is aligned with the linear actuators.

$$R_i^t = \begin{bmatrix} c\psi_i & 0 & s\psi_i \\ \theta_i s\psi_i & c\theta_i & -s\theta_i c\psi_i \\ -c\theta_i s\psi_i & s\theta_i & c\theta_i c\psi_i \end{bmatrix} \tag{5}$$

Thus, $\overrightarrow{A_i B_i})_{C_i}$ which means the description of vector $\overrightarrow{A_i B_i}$ in coordinate C_i is:

$$\overrightarrow{A_i B_i})_{C_i} = R_i^t \cdot \overrightarrow{A_i B_i} = d_i \begin{bmatrix} s\psi_i \\ -s\theta_i c\psi_i \\ c\theta_i c\psi_i \end{bmatrix} \tag{6}$$

Also we can explain q_i as follows:

$$\vec{q}_i = \vec{a}_i + R_i \cdot \overrightarrow{A_i B_i})_{C_i} \tag{7}$$

In which R_i is the transformation matrix from coordinate C_i to A.

Now we introduce the following parameters:

$$\begin{aligned} x_i &= -h\left[r_{11} c\theta_i^\circ + r_{12} s\theta_i^\circ \right] + gc\theta_i^\circ \\ y_i &= -h\left[r_{21} c\theta_i^\circ + r_{22} s\theta_i^\circ \right] + gs\theta_i^\circ \\ z_i &= -h\left[r_{31} c\theta_i^\circ + r_{32} s\theta_i^\circ \right] \end{aligned} \tag{8}$$

$$\begin{aligned} \theta_1^\circ &= -45^\circ \quad , \quad \theta_2^\circ = 45^\circ \\ \theta_3^\circ &= 135^\circ \quad , \quad \theta_4^\circ = 225^\circ \end{aligned} \tag{9}$$

Finally the desired angle θ_i can be found:

$$\theta_i = \sin^{-1}\left[\frac{s\theta_i^\circ (x - x_i) - c\theta_i^\circ (y - y_i)}{d_i c\psi_i} \right] \tag{10}$$

Equations (3) and (10) show that the mechanism has a closed form inverse kinematic solution in its workspace.

4 Forward kinematics

For the forward kinematics, 6 input to the system are given, and the position and orientation of point P are to be found.

Considering rotary and linear actuators we can obtain 3 relations from the geometry of the mechanism:

$$\begin{aligned} (\vec{q}_1 - \vec{q}_2)^T \cdot (\vec{q}_1 - \vec{q}_2) &= 2h^2 \\ (\vec{q}_1 - \vec{q}_3)^T \cdot (\vec{q}_1 - \vec{q}_3) &= 4h^2 \\ (\vec{q}_2 - \vec{q}_3)^T \cdot (\vec{q}_2 - \vec{q}_3) &= 2h^2 \end{aligned} \tag{11}$$

Replacing $\vec{q}_i$ in the joint coordinate, we can rewrite equation (11) as:

$$\begin{aligned} & e_{1i} c\psi_i c\psi_{i+1} + e_{2i} s\psi_i c\psi_{i+1} + e_{3i} c\psi_i s\psi_{i+1} + \\ & e_{4i} c\psi_{i+1} + e_{5i} s\psi_{i+1} + e_{6i} c\psi_i + e_{7i} s\psi_i + e_{8i} = 0 \end{aligned} \tag{12}$$

In which e_{ij} is a function of input variables and the geometry of the mechanism.

After using the Sylvester dialytic elimination method, the forward kinematics solution of this mechanism is reduced to a sixteen-degree polynomial. So, the forward kinematics of this mechanism has a semi-closed form solution, and there are 16 solutions at most.

5 Singularity analysis

The parallel manipulators considered here are such that the velocity relationship can be written as [9]:

$$J_x\dot{\vec{x}} = J_q\dot{\vec{q}} \quad (13)$$

Where, $\dot{\vec{x}}$ is the vector of Cartesian velocities and $\dot{\vec{q}}$ is the vector of joint velocities. The generalized velocity vector, $\dot{\vec{x}}$ is defined as the linear and angular velocity of point P. Hence, the overall jacobian matrix J_P, can be written as:

$$J_P = J_q^{-1}J_x \quad (14)$$

The Jacobian analysis of parallel manipulators is a much more difficult problem than that of serial manipulators; Because there are many links that form a number of closed loops.

Due to the existence of two jacobian matrices, a parallel manipulator is said to be at a singular configuration when either J_x or J_q or both are singular [10]. Three different types of singularities can be identified.

An inverse kinematic singularity occurs when the determinant of J_q goes to zero, namely $\det(J_q) = 0$.

J_q in this mechanism is [11]:

$$J_q = \begin{bmatrix} d_1c^2\psi_1 & 0 & 0 & 0 & 0 & 0 \\ 0 & d_2c^2\psi_2 & 0 & 0 & 0 & 0 \\ 0 & 0 & d_3c^2\psi_3 & 0 & 0 & 0 \\ 0 & 0 & 0 & 1 & 0 & 0 \\ 0 & 0 & 0 & 0 & 1 & 0 \\ 0 & 0 & 0 & 0 & 0 & 1 \end{bmatrix} \quad (15)$$

Because the determinant of J_q in this mechanism can not vanish, we do not encounter this type of singularity.

A forward kinematic singularity occurs when the determinant of J_x is equal to zero, namely

$$\det(J_x) = 0 \quad (16)$$

Hence the moving platform gains 1 or more degrees of freedom. In other words, at a forward kinematic singular configuration, the manipulator can not resist forces or moments in some directions. This kind of singularity is common in nearly all parallel mechanisms. For this mechanism J_x is equal to [11] :

$$J_x = \begin{bmatrix} (\vec{c}_1 \times \vec{l}_1)^T & (\vec{b}_1 \times (\vec{c}_1 \times \vec{l}_1))^T \\ (\vec{c}_2 \times \vec{l}_2)^T & (\vec{b}_2 \times (\vec{c}_2 \times \vec{l}_2))^T \\ (\vec{c}_3 \times \vec{l}_3)^T & (\vec{b}_3 \times (\vec{c}_3 \times \vec{l}_3))^T \\ \vec{l}_1^{\,T} & (\vec{b}_1 \times \vec{l}_1)^T \\ \vec{l}_2^{\,T} & (\vec{b}_2 \times \vec{l}_2)^T \\ \vec{l}_3^{\,T} & (\vec{b}_3 \times \vec{l}_3)^T \end{bmatrix} \quad (17)$$

As it can be seen, it is difficult to analytically identify all possible forward kinematic singularities using (16).

The main difficulty of workspace analysis for parallel robots is that a complete representation of the workspace should be embedded in a 6-dimentional space for which no direct graphical illustration is possible. Therefore, only lower dimensional subsets of the workspace can be represented.

Many types of workspace are of interest, for example the 3D constant orientation workspace, which describes all possible locations of an arbitrary point P in the moving system with a constant orientation of the moving platform, the reachable workspace (all the locations that can be reached by P), the orientation workspace (all possible orientations of the end effector around P for a given position) or the inclusive orientation workspace (all the locations that can be reached by the origin of the end effector with every orientation in a given set).

Inclusive orientation workspace, is the approach we have used here. The approach involves systematic search through a fixed work volume and evaluating the determinant of J_x. For every position in a fixed work volume, we have rotated the moving platform in every possible orientation and have determined either that configuration is a singular configuration or not. Among many transformations, it became clear that roll-pitch-yaw rotation about the fixed frame A, is more critical than the other rotations such as reduced Euler angles for determining the singularity.

As shown in Fig. 4, to avoid singularities in each of the two regions (namely blue and green) the rotations of the moving platform along the three Cartesian coordinate axes must be bounded by ±30º, ±15º, respectively. The assumed dimensions for the mechanism are $e_1 = 0.18$ m, $e_2 = 0.162$ m, $h = 0.1414$ m, $g = 0.1847$. We should note, the most critical plane in the workspace, in terms of singularities, it at the lowest elevation z=0.4m. Thus Fig. 4, represent the worst part of the workspace in terms of singularities.

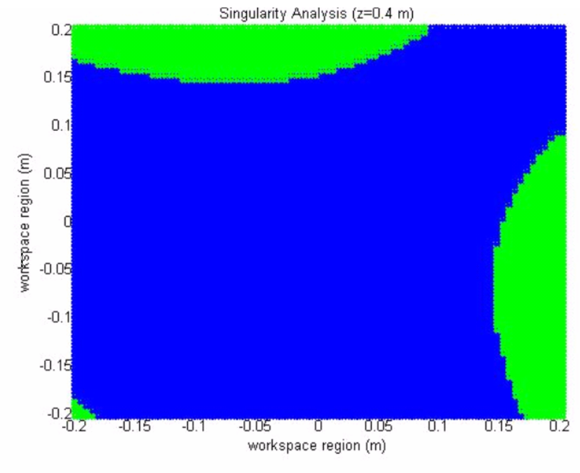

Fig. 4: Workspace singular points (critical plate)

Based on this result, it is evident that the proposed mechanism does not meet any singular points within its workspace. One should also note that since we do not have the inverse kinematic singularities in this mechanism, we do not have any the complex singularities either. This is of particular importance in haptic application and difficult maneuvers in traveling along tubular structures with bends and branches.

6 Inverse dynamics

The dynamical equations of motion can be formulated by several methods. One approach is application of the Newton and Euler laws. Another approach is application of the principle of d'Alembert or Hamilton. Alternatively, one can apply Lagrange's equations of motion or Kane's method.

The traditional Newton-Euler formulation requires the equations of motion to be written once for each body of a manipulator, which inevitably leads to a large number of equations and results in poor computational efficiency. The Lagrangian formulation eliminates all of the unwanted reaction forces and moments at the outset. It is more efficient than the Newton-Euler formulation. However, because of the numerous constraint imposed by closed loops of a parallel manipulator, deriving explicit equations of motion in terms of a set of independent generalized coordinates becomes a prohibitive task. In this regard, the principle of virtual work appears to be the most efficient method of analysis.

There are two types of dynamical problems: forward dynamics and inverse dynamics. The forward dynamics problem is to find the response of a robot arm corresponding to some applied torques and forces. The inverse dynamic problem is to find the actuator torques and forces required to generate a desired trajectory of the manipulators.

In this section we apply the principle of virtual work to derive a transformation between the joint torques and end-effector forces.

Assuming that the joints are frictionless, the reaction forces at the passive joints contribute to no virtual work.

It is well known that any system of forces and couples acting on a rigid body can be reduced to a resultant force and a couple about any point of interest. This force and couple combination is called a wrench [12].

For convenience, we introduce a six-dimensional wrench, $\hat{\vec{F}}_i$, as the sum of applied and inertia wrenches about the center of mass of link i ($\hat{\vec{F}}_{1i}$ for lower part and $\hat{\vec{F}}_{2i}$ for the upper part of the linear actuator). $\hat{\vec{F}}_{S_i}$ is the wrench of the rotary actuator, Similarly. And at last we introduce a six-dimensional wrench, $\hat{F}_p$, as the sum of applied and inertia wrenches about the center of mass of the moving platform.

Then the principle of virtual work for a parallel manipulator can be stated as [9]:

$$J_P^T\vec{\tau} + \hat{\vec{F}}_P + \sum_{i=1}^{3} J_{S_i}^T \hat{\vec{F}}_{S_i} + \sum_{i=1}^{3}\left({}^iJ_{1i}^T\,{}^i\hat{\vec{F}}_{1i} + {}^iJ_{2i}^T\,{}^i\hat{\vec{F}}_{2i}\right) = 0_{6\times1} \quad (18)$$

Note that in equation (18) we have isolated the actuator torques and forces from other applied forces for convenience of derivation. And because J_p is a 6×6 square matrix, we can uniquely determine τ :

$$\vec{\tau} = -J_P^{-T}\left(\begin{array}{l}\hat{\vec{F}}_P + \sum_{i=1}^{3} J_{S_i}^T \hat{\vec{F}}_{S_i} + \\ \sum_{i=1}^{3}\left({}^iJ_{1i}^T\,{}^i\hat{\vec{F}}_{1i} + {}^iJ_{2i}^T\,{}^i\hat{\vec{F}}_{2i}\right)\end{array}\right) \quad (19)$$

Now we summarize the procedure for solving the inverse dynamics of the proposed mechanism by using the principle of virtual work. It is assumed that the time history of the moving platform is specified in terms of the position of centroid, P, and three Euler's angles,

α, β, and γ. The velocity and acceleration of the centroid are calculated by taking the derivatives of P with respect to time. The rotation matrix of the moving platform, ${}^{A}_{B}R$, is calculated. The angular velocity and angular acceleration of the moving platform are calculated. At any instant in time, the actuator forces are computed by the following four steps:

1. Determine the position, velocity and acceleration of all links by performing the inverse kinematic analysis. Specially, for i=1 to 3, we compute:

(a) $\vec{b}_i = {}^{A}_{B}R \cdot {}^{B}\vec{b}_i$ and ${}^{A}I_P = {}^{A}_{B}R \cdot {}^{B}I_P \cdot {}^{B}_{A}R$.

(b) $\vec{d}_i$ and $\vec{c}_i$.

(c) $c\psi_i$, $s\psi_i$, $c\theta_i$, $s\theta_i$, and ${}^{A}R_i$.

(d) $\vec{v}_{bi}$ and ${}^{i}\vec{v}_{bi}$.

(e) ${}^{i}\vec{\omega}_i$.

(f) $\dot{\vec{v}}_{bi}$ and ${}^{i}\dot{\vec{v}}_{bi}$.

(g) ${}^{i}\dot{\vec{\omega}}_i$.

(h) ${}^{i}\dot{\vec{v}}_{1i}$ and ${}^{i}\dot{\vec{v}}_{2i}$.

2. Determine the platform and link Jacobian matrices.

(a) For i=1 to 3, calculate ${}^{i}J_{1i}$, ${}^{i}J_{2i}$ and then J_{S_i}.

(b) Calculate J_P.

3. Determine the resultants of the applied and inertia wrenches.

(a) Calculate $\hat{\vec{F}}_P$.

(b) For i=1 to 3, calculate ${}^{i}\hat{\vec{F}}_{1i}$, ${}^{i}\hat{\vec{F}}_{2i}$, respectively.

(c) For i=1 to 3, $\hat{\vec{F}}_{S_i}$.

4. Solve the resulting dynamical equations of motion by the Gaussian elimination method.

7 Forward dynamics

In the forward dynamics, which is more complicated than inverse dynamics, we have to convert the equation to the general nonlinear state-space form.

$$f(\vec{x}) = \dot{\vec{x}} \tag{20}$$

We summarize the procedure for solving the forward dynamics of the proposed mechanism by using the principle of virtual work. In some steps it is similar to the inverse dynamics procedure. In forward dynamics analysis, it is assumed that the three actuation forces and three actuation torques are well known. And we are intended to compute, at any instant in time, the position of centroid, P, the rotation matrix of the moving platform, the linear and angular velocities of the moving platform, through the following six steps.

1. Determine the position and velocity of all links by performing the inverse kinematic analysis. Specially, for i=1 to 3, we compute:

(a) $\vec{b}_i = {}^{A}_{B}R \cdot {}^{B}\vec{b}_i$ and ${}^{A}I_P = {}^{A}_{B}R \cdot {}^{B}I_P \cdot {}^{B}_{A}R$.

(b) $\vec{d}_i$ and $\vec{c}_i$.

(c) $c\psi_i$, $s\psi_i$, $c\theta_i$, $s\theta_i$, and ${}^{A}R_i$.

(d) $\vec{v}_{bi}$ and ${}^{i}\vec{v}_{bi}$.

(e) ${}^{i}\vec{\omega}_i$.

2. Determine the platform and link Jacobian matrices.

(a) For i=1 to 3, calculate ${}^{i}J_{1i}$, ${}^{i}J_{2i}$ and then J_{S_i}.

(b) Calculate J_P.

3. Determine the acceleration of all links by performing the inverse kinematic analysis, and then separate the coefficients of $\dot{\vec{\omega}}_P$ and $\dot{\vec{v}}_P$. Specifically for i=1 to 3 :

(a) $\dot{\vec{v}}_{bi}$ and ${}^{i}\dot{\vec{v}}_{bi}$.

(b) ${}^{i}\dot{\vec{\omega}}_i$.

(c) ${}^{i}\dot{\vec{v}}_{1i}$ and ${}^{i}\dot{\vec{v}}_{2i}$.

(d) $\ddot{\theta}_i$

4. Determine the resultants of the applied and inertia wrenches, and then separate the coefficients of $\dot{\vec{\omega}}_P$ and $\dot{\vec{v}}_P$.

(a) $\hat{\vec{F}}_P$.

(b) For i=1 to 3, ${}^{i}\hat{\vec{F}}_{1i}$ and ${}^{i}\hat{\vec{F}}_{2i}$ respectively.

(c) For i=1 to 3, $\hat{\vec{F}}_{S_i}$.

5. Replace these results in the dynamical equation of motion and convert this equation to the general state space form of nonlinear equation $f(\vec{x}) = \dot{\vec{x}}$, which $\vec{x}$ is

the six dimensional vector, namely the position and orientation of point P .

6. Solve the resulting dynamical equations of motion, by the Gaussian elimination method.

8 Simulation results

Based on the algorithm above, two computer programs were developed to solve both the inverse and forward dynamics of the proposed mechanism, using MATLAB™ software. To ensure the correctness of the programs, the simulation results have been validated using and Matlab's SimMechanics™ toolbox. The manipulator system parameters are $m_P = .3$ kg, $m_{1,i}$ =0.9 kg, $m_{2,i} = 0.4$ kg, $m_s = 0.5$ kg, $e_1 = 0.18$ m, $e_2 = 0.162$ m, $h = 0.1414$ m, $g = 0.1847$ m. The assumed inertia matrices are:

${}^{i}I_{1i} = diag[0.0097,0.0097,0]$ kg.m²,
${}^{i}I_{2i} = diag[0.0035,0.0035,0]$ kg.m²,
${}^{B}I_P = diag[0.0625,0.0625,0.125]$ kg.m² and
$I_s = diag[0.000025,0,0]$ kg.m².

The following example is solved to illustrate the forward dynamics algorithm. It is assumed that the platform starts at rest and is located 0.5 m above the fixed base, and the initial rotation angles are zero (That is at t=0, $\vec{p} = [0,0,0.5]^T$ m, ${}^{B}_{A}R = I_{3x3}$). Furthermore, it is assumed that all 3 positions and 3 orientation angles of the moving platform have a sinusoidal movement in the range of ±0.25 meter for the linear and ±0.25 rad. for the angular degrees of freedom. The period of the sinusoidal motion is assumed to be 5 seconds. The computed forces and toques are shown in fig. 5.

As expected, the period of forces and torques is also 5 s. Furthermore, all these six inputs have acceptable magnitudes.

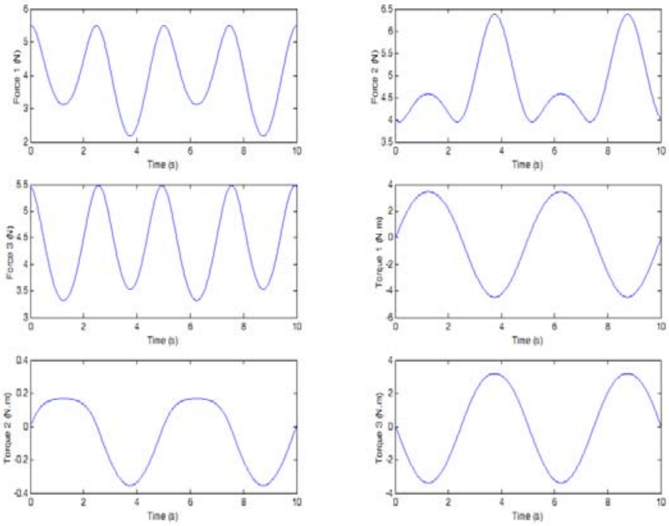

Fig. 5: Computed actuator forces and torques

9 Conclusion

A new 3 legged 6-DOF UPS parallel mechanism was introduced. High achievable accelerations due to small inertial effects, makes this mechanism ideal for haptic application. Since one side of the proposed mechanism is open, another application of this mechanism is pole climbing. The mechanism has a closed form and unique inverse kinematics solution. Forward kinematics of this robot, has at most sixteen solutions. Workspace in this mechanism is much larger than the 6 leg Stewart platform. Singularity analysis, shows that we are not encountered by critical singular points in the workspace of the mechanism. Both inverse and forward dynamics of the mechanism, are solved, using the principle of virtual work. Simulation results validate the correctness of the equations.

REFERENCES:

[1] St-Onge, B. M. and Gosselin, C. M. , 2000, "Singularity Analysis and Representation of the General Gough-Stewart Platform", *The International Journal of Robotics Research*, 19, 271-288.

[2] Fasse, E. D., Gosselin, C. M., 1999, "Spatio-Geometric Impedance Control of Gough-stewart Platforms", *IEEE Transactions on Robotcs And Automation*, 15, 281-288.

[3] Gough, V. E., Whitehall, S. G., 1962, "Universal tyre test machine", in Proc 9th Int. Tech. Congr. FISITA, 117-137.

[4] Stewart, D., 1965 "A platform with six degrees of freedom", *in Proc. Inst. Mech. Engrs*., 180-1, 371-386.

[5] Hollerbach, J. M., 2000, "Some Current Issues in Haptic Research", *Proceedings of the IEEE International Conference on Robotics & Automation*.

[6] Pouliot, N., Monsarrat, B., Birglen, L., Gosselin, C. M., Laliberté, T., 2002, "A New 3-DOF Haptic Device", *IEEE Transactions on Robotics And Automation*, 18, 166-175.

[7] Mattoccia, S., Melchiorri, C., Arcada, P., Di Stefano, L., Vassura, G., 2000 "Perception of depth information by means of a wire-actuated haptic interface", *in: Proceedings of the IEEE Internatioal Conference on Robotics And Automation*, 3443-3448.

[8] Lee, J., H., Kim, H., W., Yi, B., J., Suh, H., 2002, " Singularity-Free Algorithms and Design Scheme for A New 6-DOF Parallel Haptic Device", *in: Proceedings of the IEEE International Conference on Robotics & Automation*, 4229-4235.

[9] Tsai, L., W., 2004, " Robot Analysis", *John Wiley & Sons*.

[10] Gosselin, C. and Angeles, J., 1990, "Singularity Analysis of Closed-loop Kinematic Chains," *IEEE Trans. On Robot. Autom.,* Vol. 6, No. 3, pp. 281-290.

[11] Aghababai, O., 2005 , “Design, Kinematic and Dynamic Analysis and Optimization of a 6 D.O.F. Redundantly Actuated Parallel Mechanism for Use in Haptic Systems”, *M.Sc. Thesis, Sharif Univ. of Technology*.

[12] Roth, B., 1984, “Screws, Motors, and Wrenches That Cannot Be Bought in a Hardware Store,” *Proc. 1st International Symposium of Robotics Research*, pp.226-229.